JOURNAL OF SPACECRAFT AND ROCKETS
Vol. 31, No. 1, January–February 1994

Monte Carlo Simulation of a Near-Continuum Shock-Shock Interaction Problem

Ann B. Carlson* and Richard G. Wilmoth*
NASA Langley Research Center, Hampton, Virginia 23681

A complex shock interaction is calculated with direct simulation Monte Carlo. The calculation is performed for the type IV shock-interaction pattern produced when an incident shock impinges on the bow shock of a 0.1-in.-radius cowl lip for freestream conditions of Mach 15 and approximately 35-km altitude. Solutions are presented for a case without chemical reactions and for a full finite-rate chemistry calculation. In each case, both undisturbed flow about the cowl lip and the full shock-interaction flowfields are calculated. The differences in calculated surface properties relative to the cases with and without chemical reactions demonstrate the necessity of properly modeling the flowfield chemistry when using the analysis to predict design requirements. Preliminary grid-sensitivity studies indicate that the heat transfer predictions are conservative.

Nomenclature

d = characteristic problem dimension, m
Kn = Knudsen number
Kn' = local Knudsen number
l = gradient scale length, m
M = Mach number
P = pressure, Pa
q = heat transfer, MW/m^2
T = temperature, K
x,y = linear dimensions, m
α = macroscopic flow property
Θ = angular position measured clockwise from centerline, deg
λ = mean free path, m
ρ = density, kg/m^3

Subscripts

AXI = axisymmetric
s = stagnation
0 = undisturbed case stagnation value
2-D = two-dimensional
∞ = freestream value

Introduction

ADVANCES in computational resources in terms of CPU speed and memory, and the adoption of parallelism in some of the algorithms, have extended the applicability of direct simulation Monte Carlo (DSMC) to a limited range of continuum and near-continuum problems. This paper presents the two-dimensional simulation of the interaction of an oblique shock with the bow shock on a hypersonic inlet lip for freestream conditions of 4610 m/s velocity, -9.22×10^{-3} kg/m^3 density, and 241 K temperature. The cowl lip is noncatalytic, has a radius of 0.00254 m (0.1 in.), and has a surface temperature of 811 K. The incident shock angle is 9 deg. The impingement location of the incident shock is selected such that the localized surface heating is a maximum.

The particular shock-interaction pattern of interest is the type IV interaction[1] (see Fig. 1). This pattern involves a supersonic jet that impinges nearly normal to the surface and convects part of the high-energy stream to the surface, greatly increasing the heat transfer. The prospect of increased surface heat transfer as a result of such shock interactions is unavoidable for the hypersonic vehicle designs currently under consideration.[2] Therefore, a technique which accurately predicts the magnitude of this surface heating is required for vehicle design.

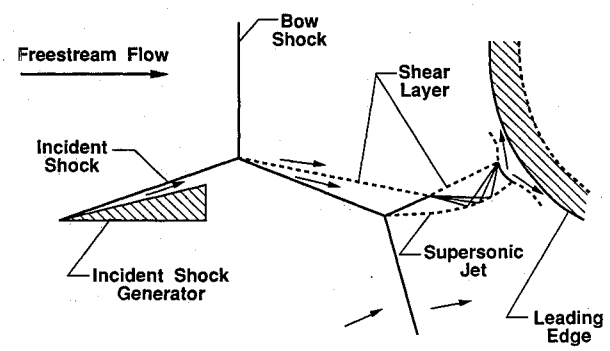

Fig. 1 Type IV supersonic jet interference pattern.

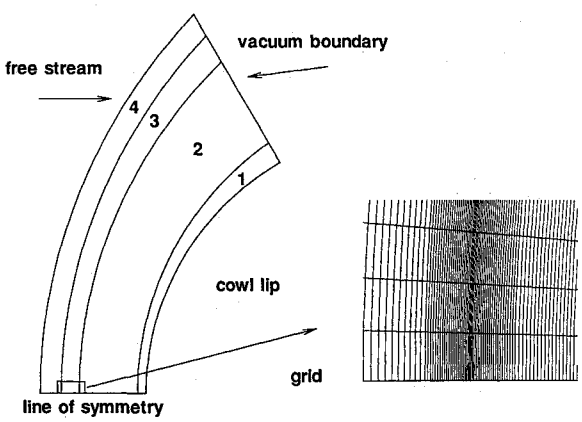

Fig. 2 Undisturbed cowl lip/bow shock geometry and grid.

Presented as Paper 92-2862 at the AIAA 27th Thermophysics Conference, Nashville, TN, July 6–8, 1992; received July 24, 1992; revision received Jan. 11, 1993; accepted for publication Jan. 12, 1993.

*Aerospace Engineer, Aerothermodynamics Branch, Space Systems Division, MS 366. Senior Member AIAA.

A primary reason for choosing to model this problem with DSMC is that the method does not depend on the continuum assumption inherent in the Navier-Stokes equations. The small cowl lip radius and relatively high altitude of the flight condition suggest that there may be some portions of the flow which are not fully within the continuum regime. A second advantage of DSMC in modeling this problem is that a full finite-rate chemical analysis can be performed without greatly increasing the computational requirements of the simulation.

Solutions of both the undisturbed flow about the cowl lip and the full shock-interaction problem are presented using both the finite-rate chemistry and near-perfect-gas (analysis performed with chemical reactions turned off) solution techniques. The near-perfect-gas solutions were obtained to facilitate comparisons with other computational fluid dynamics methods. The finite-rate chemistry computations are necessary to obtain reasonably accurate design loads for the flight condition.

Computational Method

The generalized two-dimensional direct simulation Monte Carlo code, referred to as the G2 code,[3] is used for these calculations. The unmodified G2 code is used for the undisturbed cowl lip simulations and a parallel version[4] of the code, with synchronous communication between CPUs, was used for the full shock-interaction simulations. The parallel version of the code was run using three Sun Sparcstations, each with 64 megabytes of memory. The increase in available memory through partitioning the problem across three processors allowed significantly better resolution of the flowfield than would have been possible on a single workstation.

With DSMC, each simulated molecule represents a very much larger number of real molecules. The molecular motion, intermolecular collisions, reactions, and boundary interactions are calculated for each particle as the solution is advanced by a very small time step related to the local collision frequency in the various regions. The computational grid is used to determine collision partners and for the sampling of macroscopic flow properties once a steady-state solution has been obtained. The cell sizes must be small relative to any gradients in the flowfield for an accurate solution.

The computational grid used in the undisturbed cowl bow shock simulations is shown in Fig. 2. Large flow property gradients near the cowl lip surface and in the bow shock required mesh clustering in those regions (numbered 1 and 3 on the figure). There is a freestream boundary in region 4. Molecules are reflected specularly at the line of symmetry (regions 1–4). At the cowl lip surface boundary of region 1,

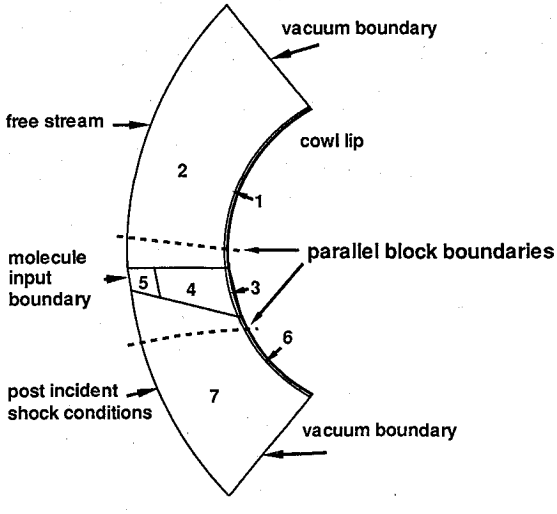

Fig. 3 Geometry and parallel block resolution for full shock-interaction problem.

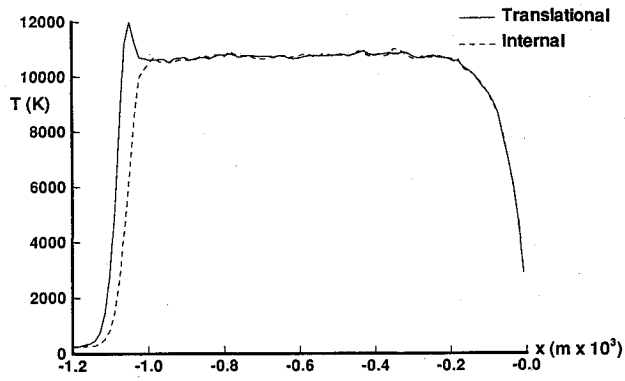

Fig. 4 Temperature along the stagnation line for near-perfect gas, undisturbed cowl lip.

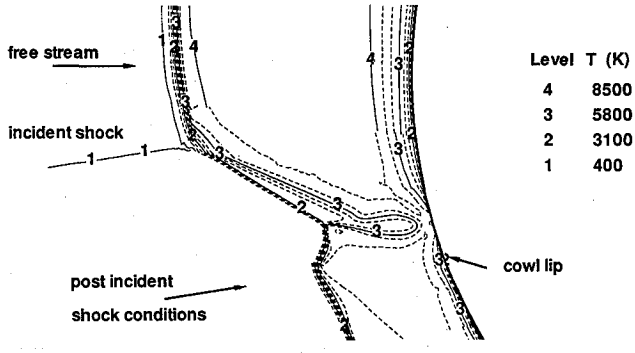

Fig. 5a Temperature contours for near-perfect-gas, shock-interaction problem.

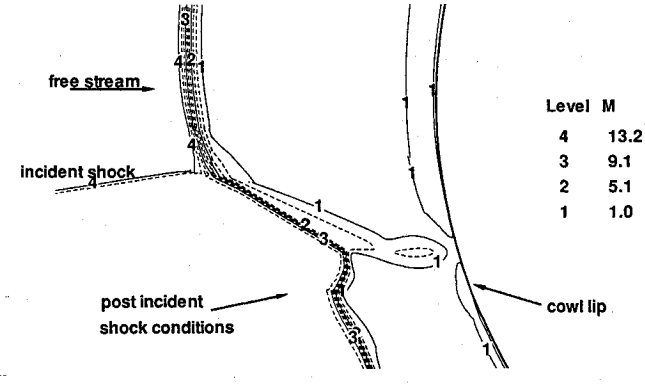

Fig. 5b Mach contours for near-perfect-gas, shock-interaction problem.

the reflection is diffuse with full surface thermal accommodation. The vacuum boundary for regions 1–4 is placed far enough from the stagnation point to assure that there is supersonic flow (Mach > 1.5) across most of this boundary, and that any errors resulting from this boundary condition will be well removed from the stagnation point, which is the region of interest. The simulations required approximately 350,000 simulated molecules, 10,000 cells, and about 600 h of CPU time on a single Sparcstation. The difference in time required between the finite-rate chemistry and near-perfect-gas solutions was not significant.

The large variation in length scales for the full interaction problem require a very complex grid. The density near the surface at the location of the supersonic jet impingement is nearly three orders of magnitude larger than the freestream density. This requires cells correspondingly smaller in this

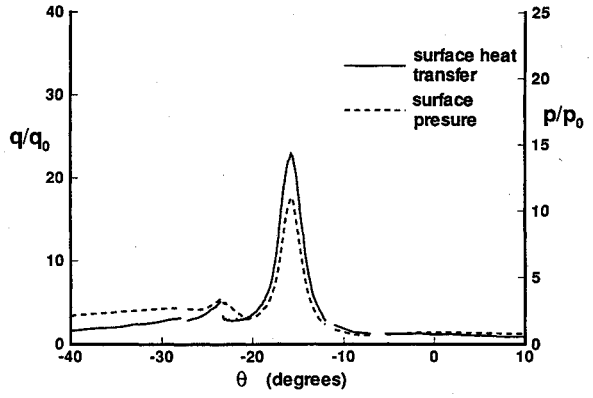

Fig. 6 Surface properties for near-perfect-gas case ($q_0 = 24$ MW/m^2, $P_0 = 1.9 \times 10^5$ Pa).

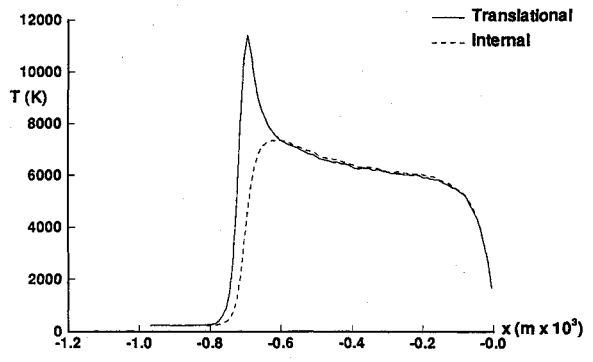

Fig. 7 Temperature along the stagnation line for finite-rate chemistry, undisturbed cowl lip.

region, particularly since the flow property gradients at this location are also large. The requirement for such a complex mesh pushes this problem beyond the limits of a single workstation. Therefore, the synchronous parallel version of the G2 code[4] was used to divide the problem among three Sun Sparcstations. Both the region breakdown (labeled 1–7) used for the solution and the decomposition for the three-processor simulation (dashed line boundaries) are shown in Fig. 3 for the finite-rate chemistry simulation. The region boundaries and processor decomposition for the near-perfect-gas case were similar. Both cases required approximately 800,000 simulated molecules, 50,000 cells, and about 3000 CPU h on each of the Sparcstations.

An important input to the full shock-interaction problem is the incident shock. This shock is input as a molecule file containing 1000 records each with 1000 ~ molecules. Molecules are introduced into the simulation randomly at each time step. The molecule input boundary is approximately 10 incident shock thicknesses long. The proper location along the molecule input boundary is preserved for each molecule in the input file, such that the full two-dimensional nature of the input shock with finite shock thickness is preserved in the simulation. Full details of the incident shock generation, and of determining the optimal incident shock location for the full shock-interaction problem, are given in Ref. 5.

Results and Discussion

Near Perfect Gas Case

Temperature along the stagnation line for the near-perfect-gas undisturbed cowl lip bow shock is shown in Fig. 4. The stagnation-point heat transfer is 24 MW/m^2 and surface pressure is 1.9×10^5 Pa. The stagnation-point heating was compared to a viscous-shock-layer (VSL), perfect-gas solution of a 20-deg sphere cone with the same radius, surface properties, and freestream conditions. A correlation for general three-dimensional stagnation points[6] was used to relate the axisymmetric VSL solution to the two-dimensional DSMC solution.

$$(q_s)_{2\text{-D}} = (q_s)_{\text{AXI}}/\sqrt{2} \tag{1}$$

This correlation is appropriate for perfect-gas flows and has been shown to give excellent results for comparisons between cylinders and spheres. The flow is in the continuum regime for the undisturbed bow shock case and the results for the two cases should be in agreement. The VSL prediction of stagnation-point heating, corrected using the preceding correlation, is 23 MW/m^2. The less than 5% difference between the two solutions is in good agreement and verifies the DSMC result.

The Mach and temperature contours for the full shock-interaction case are shown in Figs. 5a and 5b. For clarity, only a small portion of the flowfield is plotted. As can be seen from the figures, the shear layers and supersonic jet are well defined. The jet impinges in a nearly normal direction on the surface of the cowl lip and highest surface heating occurs at this point. The density near the jet impingement point is approximately 6 kg/m^3 and the maximum temperature is approximately 9000 K. The maximum surface heating is 610 MW/m^2. Surface pressure and heat transfer augmentation over the undisturbed case are presented in Fig. 6.

Finite-Rate Chemistry Case

Temperature along the stagnation line for the undisturbed cowl lip simulation is presented in Fig. 7. Note that, in comparison with Fig. 4, the shock standoff distance is less when the finite-rate chemistry is included in the modeling. Also, the temperature behind the bow shock is lower and continues to decrease through the shock layer as more dissociation occurs. The stagnation-point heat transfer is 15 MW/m^2, significantly lower than for the near-perfect-gas case, and the surface pressure is 2.0×10^5 Pa.

Mach and temperature contours for the full interaction case are shown in Figs. 8a and 8b. Besides a difference in shock standoff distance between the near-perfect-gas case and this case, the supersonic jet appears to be narrower. As can be seen in Fig. 9, this leads to a more localized heat transfer and

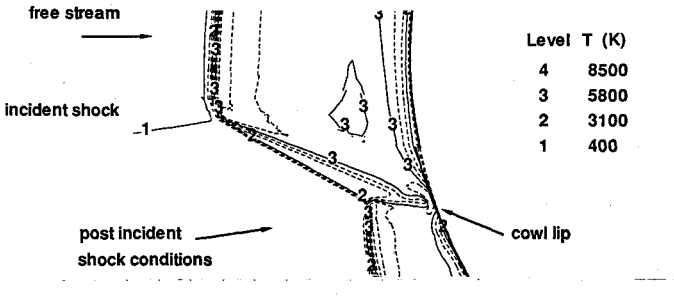

Fig. 8a Temperature contours for finite-rate chemistry, shock-interaction problem.

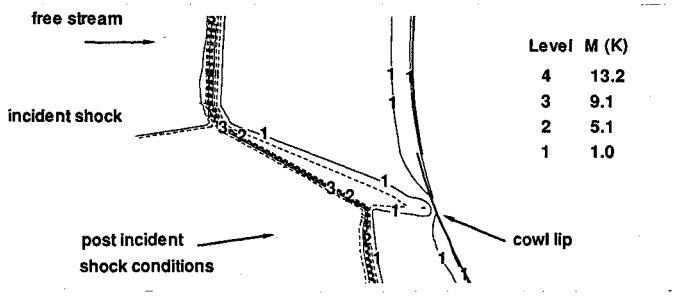

Fig. 8b Mach contours for finite-rate chemistry, shock-interaction problem.

pressure spike on the surface of the cylinder when compared to Fig. 7 for the perfect-gas case. The peak density and temperature in the gas near the jet impingement point are approximately 9 kg/m^3 and 8200 K, respectively. The maximum surface heating is 530 MW/m^2.

The distribution of chemical species across two shock-to-surface regions of the flow are shown in Figs. 10a–10c. One sample (cut A) is taken along the cowl/lip bow shock away from the interaction region. The other (cut B) is across the normal shock which occurs at the impingement location of the supersonic jet. The plots show the degree of molecular dissociation inherent in this problem. Not only is the chemistry much different across the two shocks, but comparisons of the species concentrations given in these plots with the equilibrium values for air at the same density and pressure show that the flow does not reach chemical equilibrium in either case. The chemical composition at the noncatalytic surface is also not the same at the two locations. The main difference in the composition at the surface is the amount of dissociated oxygen. The mole fraction of atomic oxygen at the jet impingement surface location is 18%, whereas it is 21% away from the jet influence. Thus, the finite-rate modeling technique is required to ensure an accurate modeling of the problem.

Grid-Sensitivity Studies

Two areas where grid resolution is critical to the accuracy of the solution are considered in some detail. The first is the area encompassing the shear layers and supersonic jet. Cells which are too large in this region would tend to smear the flow features and underpredict property gradients. This could result in an underprediction of peak surface heating by increasing the jet width but lessening the magnitude of the surface heating spike. The second area is along the surface of the cowl lip. Cells which are too large near the wall have the effect of allowing highly energetic molecules to reach the surface without undergoing the physically appropriate collisions. This tends to cause overprediction of the surface heating. Although the errors tend to be compensating, it is difficult to predict the magnitude of the error. Grid-sensitivity studies are required to determine if the grid is fine enough to provide an accurate solution.

To check the grid in the first mentioned region, a section of the flow encompassing the shear layers and the jet was modeled separately with DSMC. The effects of the cowl bow shocks and the transmitted shock were approximated by using the average properties directly behind the shocks as inflow boundary conditions, and a vacuum boundary was used at the jet exit plane (Fig. 11). As can be seen from a comparison of the Mach contours in Figs. 11 and 12, drawn to the same scale and with the same contour levels, the qualitative agreement between the solutions is excellent and the reduced version of the problem is sufficiently representative of the full version for use in grid-sensitivity studies.

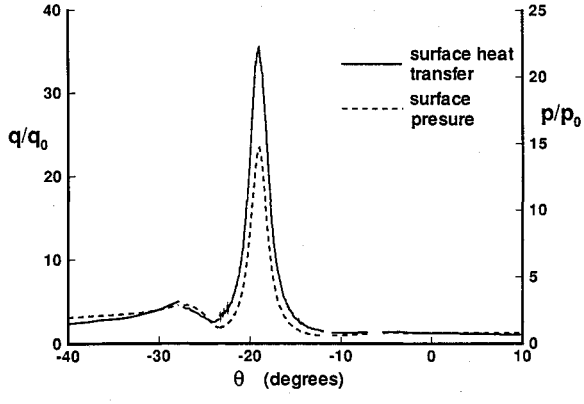

Fig. 9 Surface properties for finite-rate chemistry case (q_0 = 15 MW/m^2, $P_0 = 2.0 \times 10^5$ Pa).

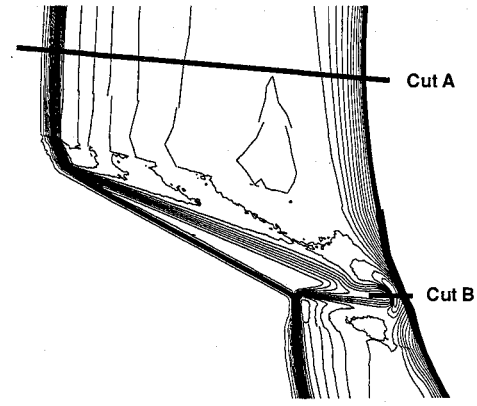

Fig. 10a Location of cuts through shocks for species-distribution plots.

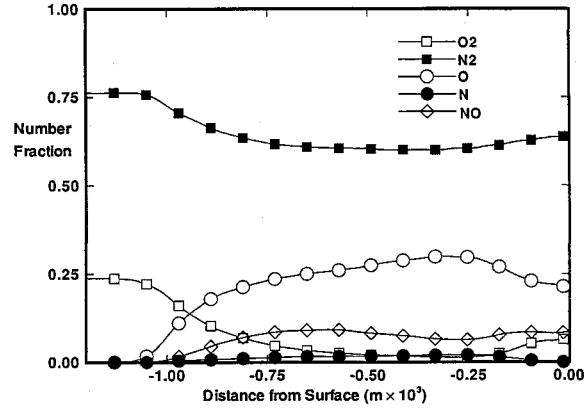

Fig. 10b Distribution of species along cut A, through cowl lip/bow shock.

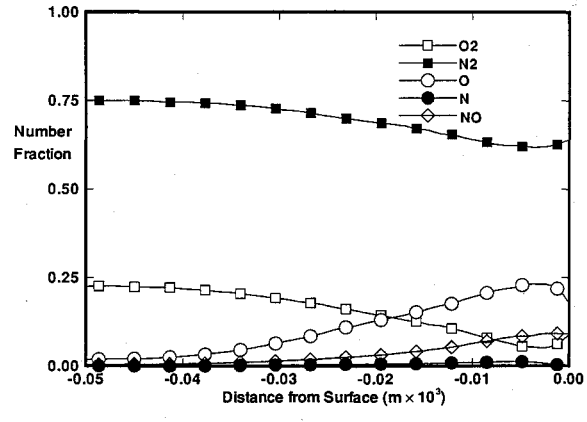

Fig. 10c Distribution of species along cut B, through jet normal shock.

The reduced problem was solved on four grids representing various levels of grid refinement in directions both parallel and perpendicular to the jet flow direction. Grid 1 represents 130 cells in the direction roughly parallel to the jet and 60 cells perpendicular to the jet (130 × 60). Grid 2 is 130 × 160, grid 3 is 50 × 160, and grid 4 is 50 × 480. Profiles of the energy flux at a location near the jet origin are presented in Fig. 13 for the four grids. There is almost no difference between the solutions for grids 2 and 3, which indicates that 50 cells in the parallel direction is adequate for the analysis. Therefore, grids 1, 2, and 4 represent adequate resolution in the parallel direction

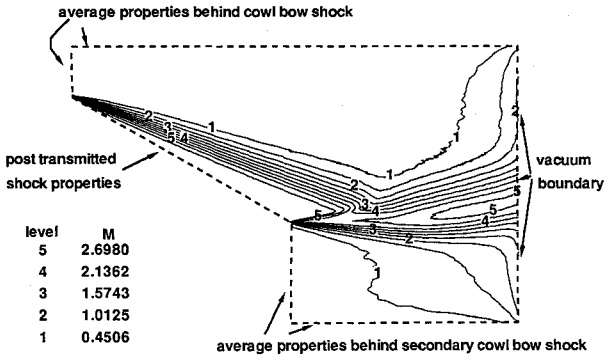

Fig. 11 Section of flowfield modeled separately for grid studies, with Mach contours.

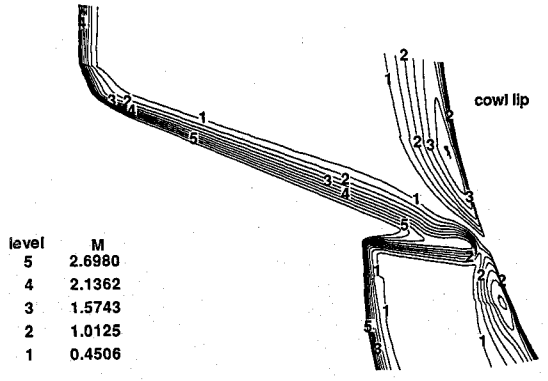

Fig. 12 Mach contours of full shock-interaction simulation for portion of the flowfield corresponding to Fig. 11.

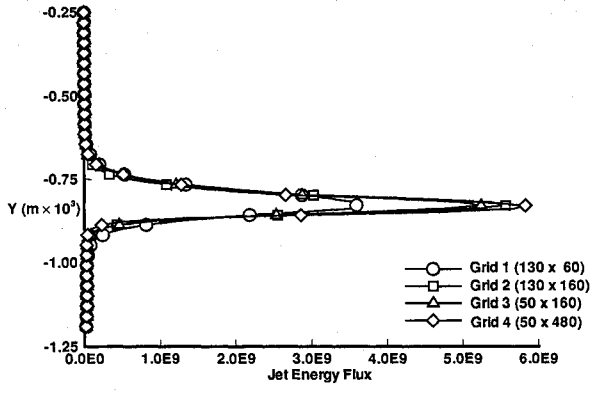

Fig. 13 Translational energy flux in the jet for four grid sizes.

and increasing resolution in the perpendicular direction. Refining the grid in the direction perpendicular to the jet produces an increasingly narrow jet with a higher peak energy flux. However, the peak energy flux is increased by 30% between grids 1 and 2 but only by about 5% between grids 2 and 4. This indicates diminishing sensitivity of the solution to grid refinement and further reductions in grid size would be expected to contribute little to the accuracy of the simulation. The full shock-interaction calculations were performed on a grid which is between grids 2 and 4 in resolution. Therefore, the grid is assumed to be adequate to predict the energy flux to the surface within at least 10% of the proper value.

The accuracy of the solution near the wall is determined by assessing the variation in properties across a cell. A good rule of thumb for DSMC calculations is that the ratio of cell size to a typical property gradient scale length should be less than 0.10 for an accurate simulation. The gradient scale length l is given by

$$l = [(1/\alpha)\ (\partial\alpha/\partial x)]^{-1} \tag{2}$$

where α is a macroscopic flow variable such as the density, velocity, or temperature. The calculated value of heat transfer to the surface is very sensitive to the grid refinement. By comparing levels of grid refinement with the calculated heat transfer at various surface locations, it was seen that the solutions were accurate to within statistical scatter as long as the ratio of cell size to density gradient scale length was less than 0.08. When the ratio was in the range 0.08 to 0.10, the heat transfer value was high by 10–20% although the surface pressure was correct. Cell sizes larger than this at the surface result in overprediction of both surface heat transfer and surface pressure. Unfortunately, it was not possible to adequately refine the grid in the immediate vicinity of the jet impingement on the surface. At this location the cells are approximately twice the desired width, and the peak heat transfer value is likely to be an overprediction.

Analysis of Noncontinuum Effects

As the capability of modeling noncontinuum flow was one justification for using DSMC for this problem, it is desirable to evaluate whether noncontinuum effects are of importance. The degree of departure of the flow from the continuum is indicated by the value of the Knudsen number. The flow Knudsen number is defined as

$$Kn = \lambda/d \tag{3}$$

Generally, the flow Knudsen number must be smaller than 0.1 for the flow to be considered in the continuum regime. However, certain portions of a flow may exhibit noncontinuum behavior even when the flow Knudsen number is smaller than 0.1. A local parameter must be selected to determine if there are noncontinuum effects in any portion of the flow. The local Knudsen number is defined as

$$Kn' = \lambda/l \tag{4}$$

where l is defined in Eq. (2). Kn' is a measure of the degree of departure from continuum for a particular location in the flowfield. Local regions of the flow are in the noncontinuum range if Kn' is greater than 0.1. For the current problem, the freestream Knudsen number based on lip radius is 0.003 and the problem would ordinarily be thought to be entirely in the continuum regime. But there are local Knudsen numbers, based on either temperature or density gradients, in the range 0.1–0.2 in portions of the flowfield which could influence the final solution (in the vicinity of the impingement of the incident shock on the cowl bow shock, in parts of the supersonic jet, and along parts of the surface). Although this indicates that the noncontinuum capability of DSMC may be required for accurate modeling of the flowfield, the question cannot be completely addressed until there are Navier-Stokes solutions of the same flight case available for comparison. The authors anticipate that such solutions will be available in the near future, at least for the perfect-gas case.

Concluding Remarks

A DSMC simulation of a complex (type IV) shock-interaction phenomena has been performed using DSMC for a flight case representative of possible trajectories under consideration for hypersonic flight vehicles. Results are presented for two cases: a near-perfect-gas representation and a nonequilibrium, finite-rate chemistry representation. The accuracy of the solution is evaluated using the results of some grid-independence studies.

Analysis of the chemistry modeling indicates that a full finite-rate capability is necessary for the prediction of the

flight-case flowfield. The amount of dissociation and the degree of chemical nonequilibrium are significant. It is also significant that the ratio of peak heating for the shock-interaction case to the undisturbed cowl stagnation heating is different when the perfect gas case is compared to the finite-rate chemistry case. This ratio, derived from wind-tunnel tests, has sometimes been used to obtain heating estimates for the flight case. The current analysis indicates that the ratio can be misleading unless the chemistry effects are considered.

The results of the simulation indicate that there may be significant noncontinuum effects which would not be adequately modeled in a typical Navier-Stokes computation. However, this question cannot be completely resolved until there are Navier-Stokes solutions of the same flight case available for comparison.

Comparison of the grid refinement in the two regions of critical sensitivity shows that the resolution of the flowfield at the wall is the most uncertain, and overprediction in heat transfer at the wall is likely to be the dominant effect. Therefore, the current solution is considered to be a conservative estimate of heat transfer to the cowl lip due to this shock-interaction phenomena.

Acknowledgments

The authors would like to express appreciation to Robert Nowak and E. V. Zoby of NASA Langley for their continued support of this research and for many helpful discussions. The assistance of R. N. Gupta also of NASA Langley, who performed the VSL analysis cited in the text, is appreciated. Also, the frequent advice and suggestions from G. A. Bird of G. A. B. Consulting Pty, Ltd. are acknowledged and appreciated.

References

[1]Edney, B., "Anomalous Heat Transfer and Pressure Distributions of Blunt Bodies at Hypersonic Speeds in the Presence of an Impinging Shock," Aeronautical Research Inst. of Sweden, FFA Rept. 115, Stockholm, 1968.

[2]Sobel, D., "Cowl Leading Edge Heat Transfer in the Presence of Shock Impingement," AIAA Paper 90-5256, Oct. 1990.

[3]Bird, G. A.,"The G2/A3 Program System Users Manual, Version 1.6," G. A. B. Consulting Pty. Ltd., Killara, NSW, Australia, Jan. 1991.

[4]Wilmoth, R. G., Carlson, A. B., and Bird, G. A., "DSMC Analysis in a Heterogeneous Parallel Computing Environment," AIAA Paper 92-2861, July 1992.

[5]Carlson, A. B., and Wilmoth, R. G., "Shock Interference Prediction Using Direct Simulation Monte Carlo," *Journal of Spacecraft and Rockets*, Vol. 29, No. 6, 1992, pp. 780–785.

[6]Hamilton, H. H., II, "Approximate Method of Calculating Heating Rates at General Three-Dimensional Stagnation Points During Atmospheric Entry," NASA TM 84580, Nov. 1982.

E. Vincent Zoby
Associate Editor